PREDICTION AND SIMULATION OF BROADBAND PROPELLER NOISE

Ali Can Takinacı[1], Tarkan Taralp[2]

ABSTRACT

An empirical prediction model of broadband noise for marine propellers is proposed. The model is composed of two components. The first component is the empirical prediction of the frequency domain broadband noise based on a well-established lifting surface algorithm providing accurate prediction of the cavitation pattern on the propeller. The second component is the modulation of the noise in the time domain. The two components of the model applied in sequence generate an output yielding a realistic propeller spectrum and audio signature. The propeller noise developed in this study, with the addition of other sources such as machinery and natural noise, is used to drive the input of a submarine sonar simulator for training purposes.

I. INTRODUCTION

Sonar operators face two critical tasks: the first is the detection of a marine vessel, and the second, the classification of the type of the vessel. The broadband noise signature emitted by the propeller section of a marine vessel plays an important role in both these tasks. Detection and classification, performed in days past only by means of headphone and a trained ear, are now supplemented though not entirely replaced by detection and classification tools such as LOFAR and DEMON.

To enhance sonar operator training sonar simulators may be employed but are limited in effectiveness by the realism of simulated signal inputs. Our work has been motivated by the desire to provide a mathematical model of the noise output of ship propellers which, assuming the addition of appropriate environmental background noise, may be used to drive the input of a sonar simulator. Both the broadband spectral shape and level, and the periodic modulating effect on the broadband noise by blade rotation is modeled so as to be amenable to spectrum analysis, DEMON analysis as well as auditory analysis by ear.

In this paper, the tonal (discrete blade rate) noise generated by the propeller blade is not modeled, as the model is limited to the broadband noise spectrum and amplitude modulation of the broadband noise spectrum for the purposes of sonar training.

The prediction of broadband noise or noise pressures radiated from marine propellers using computational or analytical methods is a relatively complicated procedure. A recent example of such procedures by making use of a time dependent panel method is reported in [7] to calculate the tonal (blade rate) noise radiated by a marine propeller operating in nonuniform wake field.

However, the prediction of broadband noise radiated from a marine propeller using empirical models is a more common approach nowadays. For recent examples of such work see [17] and [5]. These works are based on relationships similar to those used in Brown's semi empirical relation [3].

A difficulty encountered in propeller noise prediction is the limited experimental, particularly full scale measurement data available in the open literature. A recent study [1] which includes cavitation tunnel measurements as well as full scale measured data is quite valuable in this sense [15].

The primary source of propeller noise is cavitation noise generated as the propeller operates in the non-uniform wake field. The cavitation is generally composed of tip vortex and sheet cavitation. In badly designed propellers, bubble cavitation may be seen which may additionally increase the level of noise considerably. In summary, an accurate prediction of propeller cavitation in a non uniform wake field can provide a good basis upon which to predict over-all propeller noise.

In another approach, cavitation analysis on propeller blades together with the prediction of the total hydrodynamic performance may be obtained by using a verified lifting surface algorithm [14]. The approach used in this study is the model propeller concept. It can be conceptualized that the model propeller is to be tested in a cavitation tunnel. Therefore, hydrodynamic performance as well as the cavitation patterns may be obtained using a lifting surface algorithm. Using a semi empirical model, the broadband noise spectrum of the model propeller may be calculated. Adjustments may then be applied to the broadband noise spectrum to scale the results up to that of the full size propeller.

The broadband noise spectrum thus obtained represents the steady state noise spectrum generated by the propeller. To impart an extra level of realism into the model, the broadband

noise spectrum is then modulated with a blade pattern in the time domain. Sometimes this is also referred to as the "DEMON" component.

The obtained artificial propeller sound was then used as the primary input data of a submarine sonar simulator for educating naval officers.

II.   FORMULATION OF THE PROBLEM

The cavitation and performance analysis may in general be performed on marine propellers operating in non-uniform wake fields by a verified lifting surface algorithm [14].

However, direct calculation of the broadband noise is a complex procedure. The use of appropriate statistical methods is regarded to be more efficient rather than the direct calculation. In the current work, a semi empirical model similar to Brown's [3] equation is developed for the prediction of sound pressure level Ls (dB).

$$L_s = 163 + 10 \log \left[\frac{ZD^4 n_P^3}{f^2} \right] + 10 \log \left[40 \frac{A_C}{A_D} \right] + K_{Tip} \log \left[\frac{V_{Tip}}{V_{Tip}^i} \right] + 10 \log \left[H_{Dist} \right] \quad (1)$$

In the above relation Z is the number of blades, D is the diameter of the propeller (m), n_p is the rate of rotation of propeller (RPM) and f is the noise frequency (Hz). A_C and A_D represent the mean cavitation area (m²) on the blades and the propeller disk area (m²) respectively. V_{Tip} is the blade tip velocity (m/s) while V_{Tip}^i is the rotation rate (RPM) of the start of tip vortex. The value of the coefficient K_{Tip} is normally taken to be 60. But for deeply submerged propellers (e.g. submarine propeller) a value of 80 is suggested in [11]. H_{Dist} is the hydrophone placement distance (m) from the model propeller in the cavitation tunnel.

In Equation (1) both the effect of sheet cavitation and tip vortex cavitation are included based on the model propeller characteristics in a cavitation tunnel. However, it must be born in mind that, the inception of tip vortex cavitation depends not only on cavitation number, but also on Reynolds number as indicated e.g. in reference [2]. This means, if the noise spectrum in model scale will be extrapolated to those in full scale, the part for unsteady sheet cavitation and tip vortex cavitation must be treated separately. But the Equation (1) developed (or proposed) here is purely empirical and the effect of tip vortex together with sheet cavitation are included to reflect the logical sequence of the development of sheet cavitation although the scaling of the tip vortex in the above formula will be subject to Reynolds number effect.

Equation (1) is valid for f_p<10 kHz where the center frequency f_p lies at the peak of the broadband noise spectrum. In the present study, f_p is determined using the formulae

$$f_p = \frac{4400}{D} \left(\frac{\sigma_n^i}{\sigma_n} \right)^{-3.2/2} \left(\frac{P_s}{22} \right)^{1/3} \Rightarrow \left(\frac{\sigma_n^i}{\sigma_n} \right)^{1/2} < 1.7$$

$$f_p = \frac{1100}{D} \left(\frac{\sigma_n^i}{\sigma_n} \right)^{-2.0/6} \left(\frac{P_s}{22} \right)^{1/3} \Rightarrow \left(\frac{\sigma_n^i}{\sigma_n} \right)^{1/2} \geq 1.7$$

$$(2)$$

which are commonly utilized in connection with pump cavitation [12]. Here, P_s is the static pressure (lbs/in²), and σ_n is the

cavitation number which is defined as

$$\sigma_n = \frac{P_s - P_V}{\frac{1}{2} \rho n_P^2 D^2} \quad (3)$$

where P_V is the vapor pressure of water (1700–2400 Pa) and σ_n^i is the incipient cavitation number derived from

$$\frac{A_C}{A_D} = \left[\left(\frac{\sigma_n^i}{\sigma_n} \right)^{1/2} - 1 \right]^2 \left(\frac{\sigma_n^i}{\sigma_n} \right)^{-1} \quad (4)$$

Equation (1) determines the sound pressure level at the peak frequency where $f = f_p$. Otherwise, the sound pressure level is obtained by

$$L_s = A f^{0.007} \Rightarrow f < f_p$$
$$L_s = B f^{-0.2} \Rightarrow f > f_p$$
$$(5)$$

Here, the constants A and B are determined from the continuity characteristics of the noise spectrum and they are given by

$$A = \left(\frac{L_{s_p}}{f_p} \right)^{0.007} ; \quad B = \left(\frac{L_{s_p}}{f_p} \right)^{-0.2} \quad (6)$$

The sound pressure level L_{s_p} is obtained from the use of Equation (1) for the peak frequency f_p. Hence, Equation (5) together with Equation (1) yields a broadband noise spectrum over the frequency range of interest.

III.   SCALING

The present work is carried out assuming scale model propellers compatible with the dimensions of Emerson Cavitation Tunnel at University of Newcastle. The goal is to predict the noise spectrum of a 30 cm diameter propeller. Under these conditions the hydrophone distance H_{Dist} from model is taken to be 0.435 m.

Later, an approximation to the full-scale noise levels is carried out using the scaling laws recommended by the Cavitation Committee in of ITTC [6]. The increase in the noise level in moving from model to full scale is given by,

$$\Delta L_{(P)} = 20 \log \left[\left(\frac{D_P}{D_M} \right)^z \left(\frac{r_M}{r_P} \right)^x \left(\frac{\sigma_P}{\sigma_M} \right)^{y/2} \left(\frac{n_P D_P}{n_M D_M} \right)^y \left(\frac{\rho_P}{\rho_M} \right)^{y/2} \right] dB \quad (7)$$

and the frequency shift is expressed as (see [6])

$$\frac{f_P}{f_M} = \frac{n_P}{n_M} \quad (8)$$

In the above equations, the subscripts P and M refer to the full-scale and the model scale respectively, r is the reference distance at which the noise level is predicted, prescribed as 1 m for both the full-scale and the model scale calculations. σ is the cavitation number taken to be the same value for both the full-scale and model, n is the propeller rate of rotation and ρ is the mass density of water assumed to be 1000 kg/m³ for the scale model in the cavitation tunnel conditions and 1025.9 kg/m³ for the full scale propeller in the sea water conditions. Furthermore, setting $y=2$ and $z=1$, the expression for the increase in the noise level reduces to

$$\Delta L_{(P)} = 20 \log \left[1025.9 \lambda^3 \left(\frac{n_P}{n_M} \right)^2 \right] dB \tag{9}$$

The parameter λ is the scale ratio between the model (30 cm diameter) and the full-scale propellers.

IV. PROPELLER DEMON COMPONENT

Once a broadband noise model has been established for the propeller under study, a modulation model can be developed to impart a realistic time domain signature to the broadband noise model. This is sometimes referred to as the "DEMON" component [8], [9]. As the propeller blade rotates about the shaft axis it passes through different regions of wake flow and turbulence, which results in cavitation and associated peaks in generated noise. The cavitation noise envelope exhibits both cyclical and random components which may be attributed to the wake flow pattern and to the turbulence in the wake flow. This gives rise to a cavitation noise amplitude, or envelope, which continually varies as the propeller rotates about the shaft axis [13]. The cyclical variation of the propeller cavitation noise envelope is modeled as a form of amplitude modulation by Lourens [9] by Kummert [8] and by Nielsen [10]. The authors of the cited papers utilize the amplitude modulation model for the purpose of analyzing observed real propeller signals.

In this work, the aim is to synthesize an artificial propeller signal. In order to generate the artificial signal, the propeller noise spectrum obtained in the previous section is used as input. The propeller noise spectrum may be represented by the N-point discrete frequency domain function $X(k)$. The frequency index k is related to actual frequency by the relation

$$f = \begin{cases} k \cdot f_s / N, & 0 \le k \le N/2 \\ (N-k) \cdot f_s / N, & N/2 < k < N \end{cases} \tag{10}$$

$X(0)$ corresponds to the DC (zero frequency) component of the spectrum and $X(N/2)$ corresponds to the Nyquist frequency $f_s/2$. The remaining components are complex conjugates of one another such that $X(N-k) = X^*(k)$.

To simulate a natural time domain signal, a random phase is associated with the spectral value $X(k)$ which results in the randomized spectral value $X_r(k)$. The random phase is generated using a uniform random variable U on the interval $[0,1)$.

$$X_r(k) = \begin{cases} X(k) & k = 0, k = \frac{N}{2} \\ X(k) e^{2\pi i U} & 0 < k < \frac{N}{2} \\ X_r^*(N-k) & \frac{N}{2} < k < N \end{cases} \tag{11}$$

The time domain signal of the broadband noise is attained by taking the discrete Fourier transform of the randomized frequency spectrum. In other words,

$$x(n) = DFT\{X_r(k)\} \text{ Pa} \tag{12}$$

The modulator function m(t) is a sum of sinusoids and harmonics in the form of a Fourier series,

$$m(t) = \sum_{n=0}^{\infty} A_n \cos(n 2\pi f_{shaft} t) \tag{13}$$

$$f_{shaft} = n_P / 60$$

The coefficients of the sinusoidal modulating function and its harmonics are represented by the coefficients $A_0, A_1, ..., A_\infty$.

Coefficient A_0 is the average (DC) value of the modulator function. Coefficient A_1 is the magnitude of the sinusoid of the shaft turn rate frequency f_{shaft}. The coefficients $A_2, A_3, ...,$ are the magnitudes of the harmonics of the shaft frequency.

The time domain broadband noise $x(n)$ Equation (12) is modulated with the modulator function $m(t)$ Equation (13) to produce the final output signal $y(n)$. Given that $t = n/f_s$ the function $m(t)$ may also be written as $m(n/f_s)$. Thus the resulting modulated propeller noise $y(n)$ is given by

$$y(n) = m(n/f_s) \cdot x(n) \text{ Pa} \tag{14}$$

Various constraints need to be introduced to the above mentioned parameters. In order to ensure a well formed modulation, the constant coefficient A_0 should be greater than the sum of the other coefficients. Furthermore, in order to ensure that the modulation does not create a change in average power level of the signal, the sum of the coefficients squared must equal unity. Thus,

$$A_n \ge 0$$

$$A_0 = \frac{1}{\alpha} \sum_{n=1}^{\infty} A_n, \quad 0 < \alpha \le 1 \tag{15}$$

$$1^2 = A_0^2 + \frac{1}{2} \sum_{n=1}^{\infty} A_n^2$$

The coefficient α controls the modulation level, which adjusts the variation in amplitude about the mean level.

The determination of the harmonic coefficients A_k is relatively more complex. The ship propeller noise typically exhibits a strong harmonic at the blade frequency f_{br} defined as

$$f_{br} = k \frac{n_P Z}{60} Hz \tag{16}$$

$$k = 1,2,3,...$$

Hence the value for the coefficient A_Z is typically greater than the other coefficients.

V. NUMERICAL EXAMPLE

The developed model is applied to a four bladed propeller whose principal dimensions are provided in Table 1. The offsets of the blade sections and the hub as well as the details of the trailing and leading edges of the blades are obtained from [15].

Table 1. Main Particulars of the Propeller.

Number of Blades	4
Propeller Diameter (m)	2.100
Pitch Ratio at 0.7R	0.8464
Expanded Blade Area Ratio	0.55
Boss Ratio	0.276
Rake	0
Skewback (degrees)	40
Direction of Rotation	Right Handed

The 3D representation of the propeller is provided in Figure 1. The non-uniform wake field in which the propeller operates is shown in the form of a velocity ratio contour plot in Figure 2.
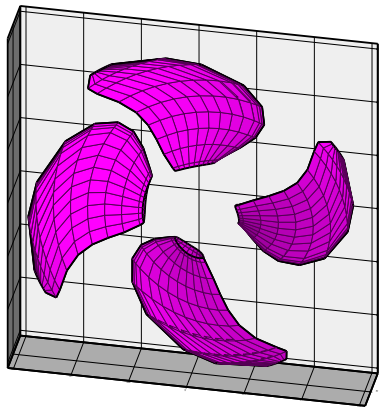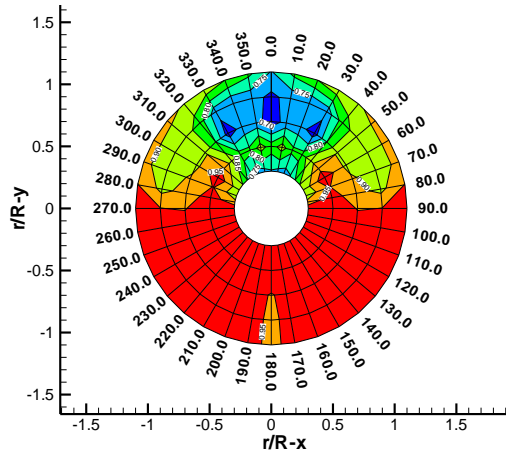
Fig. 1. 3D Representation of Propeller.

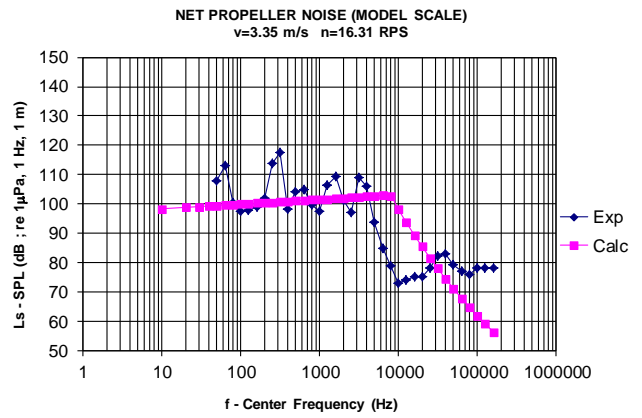**Fig. 2. Non Uniform Wake Field in terms of Velocity Ratios.**

Fig. 3. Model Propeller Broadband Noise Spectrum for Condition 1 in Table 2.

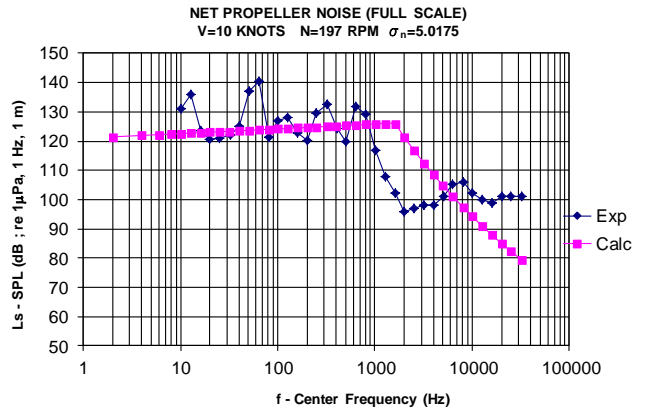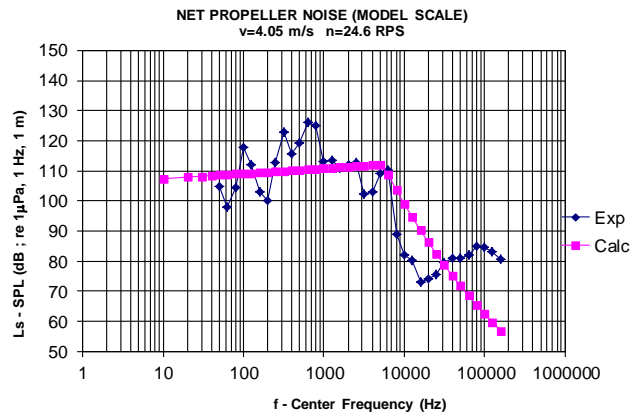**Fig. 4. Full Scale Propeller Noise Level for Condition 1 in Table 2.**

Fig. 5. Model Propeller Broadband Noise Spectrum for Condition 2 in Table 2.

The sample test conditions based upon the cavitation tunnel test obtained from [15] are outlined in Table 2.

The predicted and measured sound pressure spectrum levels for the test conditions in Table 2 are presented in Figures 3 and 5 for the model and in Figures 4 and 6 for the full-scale propeller. In these figures, the logarithmically scaled x-axis represents the center frequencies (f) in Hz while the linearly scaled y-axis represents the sound pressure levels (L_s) in dB re 1 μPa, 1 Hz, 1 m. A common practice in the analysis and presentation of the noise levels is to reduce the values of Sound Pressure Levels – L_s (SPL) in each 1/3 Octave band to an equivalent 1 Hz band-width.

Table 2. Full-scale and Corresponding Test Conditions for Noise Modeling.

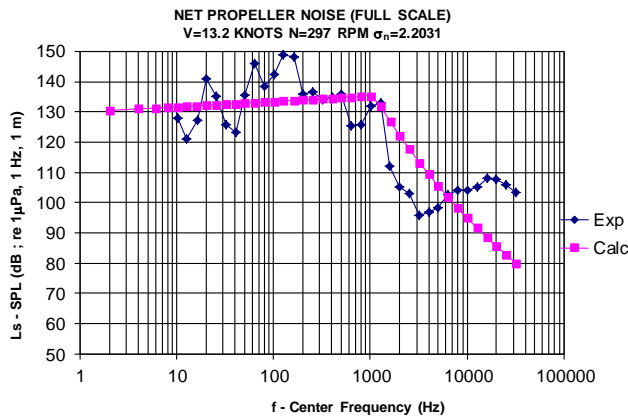| Condition No	Ship's Speed (knots)	σ_n	n_M	Tunnel Speed v (m/s)
1	10.0	5.0175	978	3.35
2	13.2	2.2031	1476	4.05

Fig. 6. Full Scale Propeller Noise Level for Condition 2 in Table 2.

Figures 3 through 6 compare the experimentally measured and the predicted noise levels. The curve consisting of two relatively smooth sections is the predicted spectrum. The other curve shows the experimentally measured spectrum. The predictions are in fairly good agreement with the experimental data.

Having established a broadband noise spectrum prediction, the next step is obtaining an audio model by modulating the broadband noise spectrum. The generated propeller broadband noise for Condition 1 (Table 2) is modulated by the procedure described previously using the parameters listed in Table 3. The determination of the harmonic coefficients A_k of the modulator function is not straightforward, and is there is a lack of empirical study of the parameters associated with amplitude modulated propeller noise in the literature [10]. Nevertheless as a general principle, for a Z blade propeller, the Zth harmonic component is expected to be dominant. Typical to commercial propellers, one blade exhibits significantly higher cavitation than the other blades resulting in a rhythmic pattern which may be detected by ear or on a DEMON graph. Thus the first harmonic is also expected to be dominant relative to the others. Based on these heuristics, and in consultation with sonar personnel, a set of parameters was chosen which reasonably simulated both the auditory sound effects of, as well as the expected output of DEMON analysis, of a civilian cargo vessel propeller.

Table 3. Propeller Noise Modulator Harmonic Input Values.

n_p	197
Z	4
α	0.5
A_0	0.986295
A_1	0.108666
A_2	0.051330
A_3	0.051330
A_4	0.179160
A_5	0.051330
A_6	0.051330

The time domain version $x(n)$ of the spectrum from Figure 4 (Condition 1) is attained using Equation (12), and the result is shown in Figure 7. The graph of $x(n)$ is limited to a one second period for the purpose of clarity.
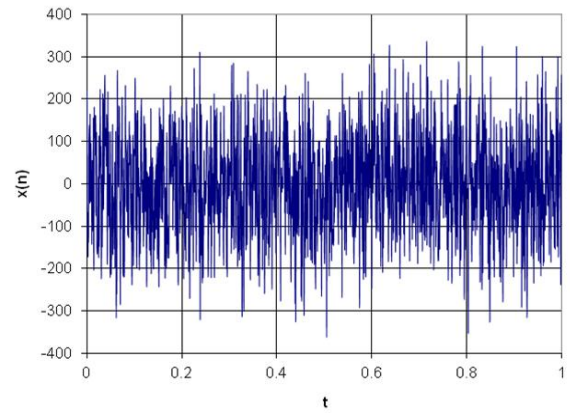

Fig. 7. Broadband Noise (Time Domain Version of Spectrum).

The modulator function $m(t)$ defined in Equation (14) is used to modulate the broadband noise signal in order to simulate the propeller noise. The parameters in Table 3 are used in Equation (13). The resulting function $m(t)$ is shown in Figure 8.
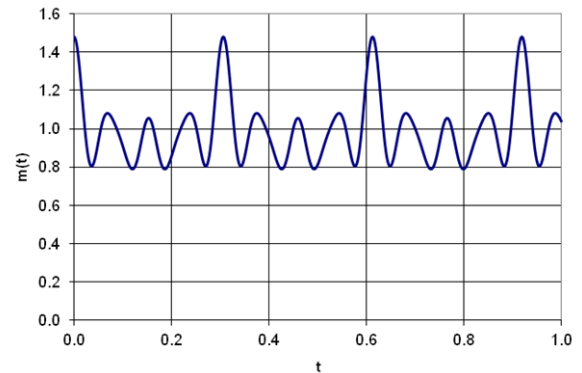

Fig. 8. Modulator Function.

By modulating the broadband noise $x(n)$ with the modulator function $m(t)$ as shown in Equation (14) the output propeller signal $y(n)$ is obtained. As can be seen in Figure 9, the amplitude of the original broadband noise $x(n)$ varies with the peaks introduced by the modulator function $m(t)$.
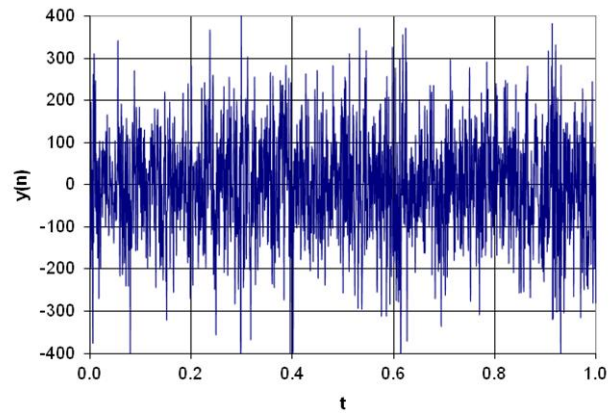

Fig. 9. Propeller Modulated Noise.

It is concluded that the empirical prediction of broadband noise followed by a modulation technique as outlined in this work may be used to generate a realistic time series audio signal. The full audio signal in WAV or MP3 format may be downloaded from the web site [16].

VI. CONCLUSIONS

An empirical prediction model of broadband noise for marine propellers is developed. The model is composed of two components: firstly, the empirical prediction of the frequency domain broadband noise, and secondly, modulation of the noise in the time domain.

The results of the empirical prediction model are seen to be in general agreement with the available experimental data. In order to impart a realistic audio character to the spectrum thus obtained, a modulation model is also employed. As a result the data obtained in the frequency domain is converted into an audible output.

For the future work, it is desired to enrich the empirical prediction algorithm and the modulation parameters further with more empirically gathered data.

NOMENCLATURE

A, B	Constants (Defined in Eq. (6))
A_{0-n}	Constants in Eq.(15)
A_c	Mean Cavitation Area on Propeller Blades (m^2)
A_D	Propeller Disk Area (m^2)
D	Diameter of Propeller (m)
K_{Tip}	Constant (Either 60 or 80)
L_s	Sound Pressure Level (dB)
L_{S_P}	Value of Sound Pressure Level for Peak Freq. (dB)
N	Number of Points in Fourier Transform (Eq. 10)
P_s	Static Pressure (Psi in Eq.(2), Pa in Eq.(3))
P_v	Vapor Pressure (Pa)
V_{Tip}	Tip Speed of Propeller Blade (m/s)
V_{Tip}^i	Rotation Rate of Start of Tip Vortex (RPM)
$X(k)$	Spectral Value of Broadband Noise at Freq. Index k
$X_r(k)$	Spectral Value with random phase
Z	Number of Propeller Blades
f	Noise Frequency (Hz)
f_{br}	Propeller Blade Rate Frequency (Hz)
f_p	Center Frequency (Hz)
f_s	Sample Frequency (Hz)
f_{shaft}	Shaft Frequency (Hz) (Eq.(13))
$m(t)$	Modulator Function (Eq. (13))
n_p	Rotation Rate of Propeller (RPM)
k	Frequency Index (Defined in Eq. (10))
r	Propeller Radius (m)
$x(n)$	Broadband noise time domain function (Eq.(12))
$y(n)$	Final Output Signal (Pa) (Eq.(14)
P,M	Indices for full scale propeller and its model
$\Delta L_{(P)}$	Frequency Shift in Eq. (7) (dB)
λ	Model Scale Ratio (Diameter of model propeller is always taken as 30 cm)
ρ	Density of Fluid (kg/m^3)
σ_n	Cavitation Number
σ_n^i	Incipient Cavitation Number

REFERENCES

1. Atlar, M., Takinacı, A.C., Korkut, E., Sasaki, N., and Aono, T., "Cavitation Tunnel Tests for Propeller Noise of a FRV and Comparisons with Full-Scale Measurements," presented at *CAV 2001: Fourth International Symposium on Cavitation*, Pasadena, USA, June 20-23 (2001).
2. Blake, W.K. "Propeller Cavitation Noise: The Problems of Scaling and Prediction," *ASME Symposium on cavitation and Multiphase Flow Noise* (1986).
3. Brown, N.A., "Cavitation Noise Problems and Solutions", *International Symposium on Shipboard Acoustics* (1976).
4. Carlton, J.S., *Marine Propellers and Propulsion*, 2nd ed., Butterworth Heinemann (2007).
5. Hazelwood, R.A. and Conelly J., "Estimation of Underwater Noise – A Simplified Method," *Int. Journal of the Society for Underwater Technology*, vol. 26, no. 3, pp. 97-103, Nov. (2005).
6. ITTC, "Cavitation Committee Report", *18th International Towing Tank Conference*, Kobe, Japan (1987).
7. Kehr, Y.Z. and Kao, J.H., "Numerical Prediction of the Blade Rate Noise Induced by Marine Propellers," *Journal of Ship Research*, vol. 48, no. 1, pp. 1-14, March (2004).
8. Kummert, A., "Fuzzy Technology Implemented in Sonar Systems," *IEEE J. Oceanic Eng.*, vol. 18, no. 4, pp. 483-490, Oct. (1993).
9. Lourens, J.G and du Preez, J.A., "Passive Sonar ML Estimator for Ship Propeller Speed," *IEEE J. Oceanic Eng.*, vol. 23, no. 4, pp. 448-453, Oct (1998).
10. Nielsen, R.O., "Cramer-Rao Lower Bounds for Sonar Broad-Band Modulation Parameters," *IEEE J. Oceanic Eng.*, vol. 24, no. 3, pp. 285-290. July (1999).
11. Odabaşı, A.Y., *Cavitation Inception and Prediction of Broad-Band Noise Levels*, British Maritime Technology, Tech. Rep. W1607, March (1987).
12. Okamura, N. and Asano, T., "Prediction of Propeller Cavitation Noise and Its Comparison with Full-Scale Measurements," *Journal of the Society of Naval Architects of Japan*, vol. 164 (1988).
13. Ross, D., *Mechanics of Underwater Noise*, Peninsula Publishing, pp. 253-285 (1987).
14. Szantyr, J.A., "A Method for Analysis of Cavitating Marine Propellers in Non-uniform Flow," *International Shipbuilding Progress*, vol. 41, no. 427, pp. 223–242 (1994).
15. Takinacı, A.C., Korkut, E., Atlar, M., Glover, E.J., Paterson, I., *Cavitation Observation and Noise Measurements with Model Propeller of a Fisheries Research Vessel*, Dept. of Marine Technology, Univ. of Newcastle upon Tyne, UK, Report MT-2000-56 (2000).
16. Takinacı, A.C., Propeller Noise Simulation Web Page. [Online] Available: http://www.gidb.itu.edu.tr/staff/takinaci/NoiseSimulation/PropNoiseSimulation.html, (2008).
17. Yoshimura, Y. and Koyanagi, Y., "Design of a Small Fisheries Research Vessel with Low Level of Underwater-Radiated Noise," *Journal of the Marine Acoustics Society of Japan*, vol. 31, no. 3, pp. 137-145 (2004).